The Journal of Experimental Biology 209, 3569-3579
Published by The Company of Biologists 2006
doi:10.1242/jeb.02486

Frictional adhesion: a new angle on gecko attachment

K. Autumn[1,*], A. Dittmore[1], D. Santos[2], M. Spenko[2] and M. Cutkosky[2]

[1]*Department of Biology, Lewis & Clark College, 0615 SW Palatine Hill Road, Portland, OR 97219, USA and*
[2]*Department of Mechanical Engineering, Stanford University, Building 530, 440 Panama Mall, Stanford, CA 94305-3030, USA*

*Author for correspondence (e-mail: autumn@lclark.edu)

Accepted 11 August 2006

Summary

Directional arrays of branched microscopic setae constitute a dry adhesive on the toes of pad-bearing geckos, nature's supreme climbers. Geckos are easily and rapidly able to detach their toes as they climb. There are two known mechanisms of detachment: (1) on the microscale, the seta detaches when the shaft reaches a critical angle with the substrate, and (2) on the macroscale, geckos hyperextend their toes, apparently peeling like tape. This raises the question of how geckos prevent detachment while inverted on the ceiling, where body weight should cause toes to peel and setal angles to increase. Geckos use opposing feet and toes while inverted, possibly to maintain shear forces that prevent detachment of setae or peeling of toes. If detachment occurs by macroscale peeling of toes, the peel angle should monotonically decrease with applied force. In contrast, if adhesive force is limited by microscale detachment of setae at a critical angle, the toe detachment angle should be independent of applied force. We tested the hypothesis that adhesion is increased by shear force in isolated setal arrays and live gecko toes. We also tested the corollary hypotheses that (1) adhesion in toes and arrays is limited as on the microscale by a critical angle, or (2) on the macroscale by adhesive strength as predicted for adhesive tapes. We found that adhesion depended directly on shear force, and was independent of detachment angle. Therefore we reject the hypothesis that gecko toes peel like tape. The linear relation between adhesion and shear force is consistent with a critical angle of release in live gecko toes and isolated setal arrays, and also with our prior observations of single setae. We introduced a new model, frictional adhesion, for gecko pad attachment and compared it to existing models of adhesive contacts. In an analysis of clinging stability of a gecko on an inclined plane each adhesive model predicted a different force control strategy. The frictional adhesion model provides an explanation for the very low detachment forces observed in climbing geckos that does not depend on toe peeling.

Key words: gecko, adhesion, friction, tribology, contact mechanics, biomechanics, robotic.

Introduction

Tokay gecko feet have five highly flexible digits, each bearing toe pads consisting of arrays of hundreds of thousands of microscopic setae (Fig. 1). Each seta splits into hundreds of 200 nm wide spatular tips. In their resting state, setal stalks are angled, and recurved proximally. When the toes of the gecko are planted, the setae bend out of this resting state, flattening the stalks between the toe and the substrate such that their tips point distally. This small preload and a μm-scale displacement of the toe or scansor proximally may serve to bring the spatulae (previously in a variety of orientations) uniformly flush with the substrate, maximizing their surface area of contact. Adhesion in isolated setae requires a small push perpendicular to the surface, followed by a small parallel drag (Autumn et al., 2000). When properly oriented, preloaded and dragged, a single seta can generate 200 μN in shear (Autumn et al., 2000) and 40 μN in adhesion (Autumn et al., 2002), over three orders of magnitude more than required to hold the animal's body weight (Autumn and Peattie, 2002). Given the surprisingly large forces generated by single setae one wonders how geckos manage to detach their feet in just 15 ms (Autumn et al., 2006a) with no measurable detachment forces.

Microscale detachment of setae at 30°

At the microscale, detachment can be accomplished by increasing the angle that the setal shaft makes with the substrate above 30° (Autumn et al., 2000). This is consistent with models of setae as cantilever beams (Autumn, 2006; Autumn et al., 2006b; Gao et al., 2005; Sitti and Fearing, 2003; Spolenak et al., 2005) and with finite element modeling of the seta (Gao et al., 2005). It is likely that as the angle of the setal shaft increases, sliding stops and stress increases at the trailing edge

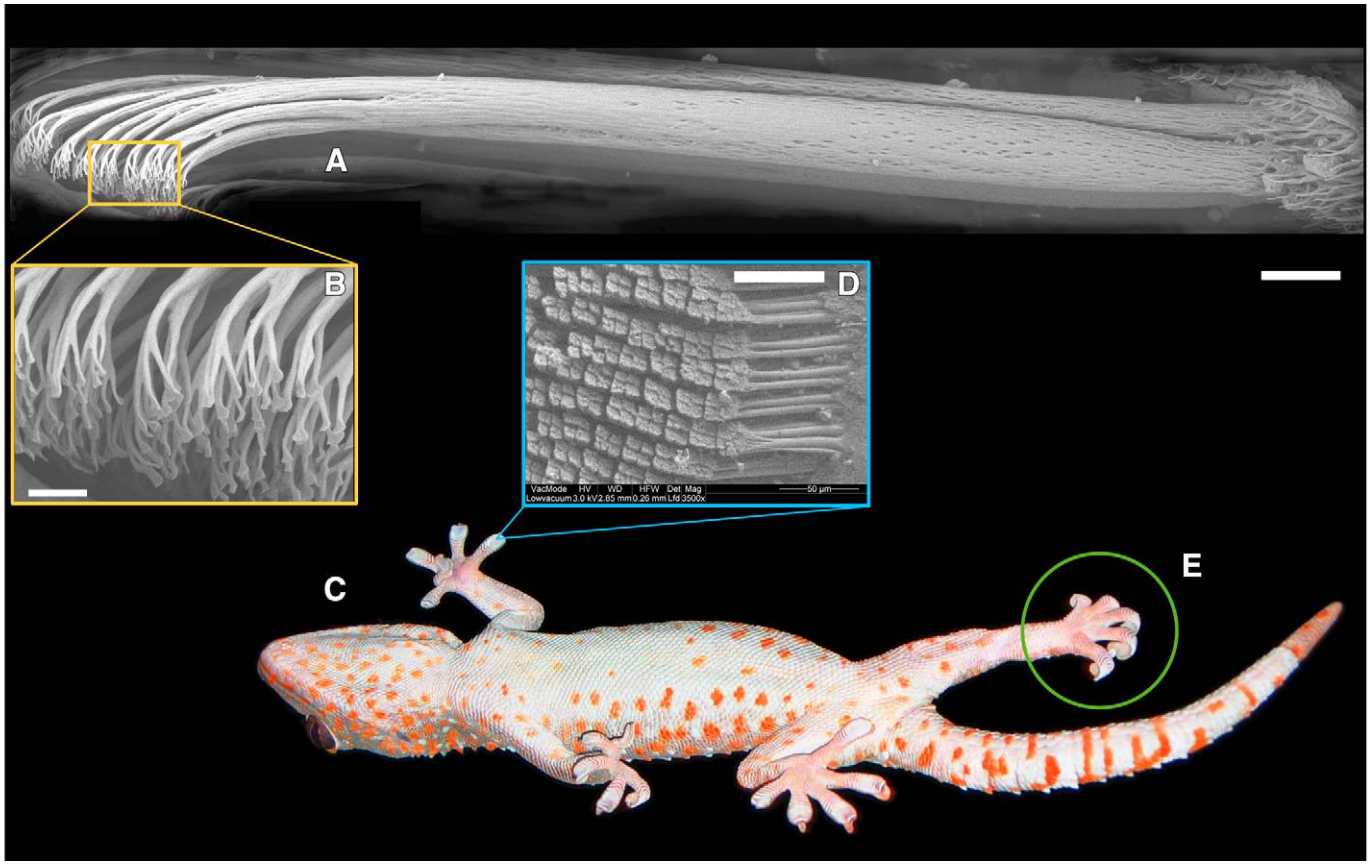

Fig. 1. Gecko adhesive system. (A) Micrograph of a single gecko seta assembled from a montage of five Cryo-SEM images (image by Stas Gorb and K. Autumn). (B) Nanoscale array of hundreds of spatular tips of a single gecko seta. Note that the field of spatulae forms a plane at an acute angle to the base of the setal shaft. Raising the angle of the shaft above 30° may cause spatular detachment (Autumn et al., 2000; Gao et al., 2005). (C) Ventral view of a tokay gecko (*Gekko gecko*) climbing a glass surface. (D) Array of setae are arranged in a nearly grid-like pattern on the ventral surface of each scansor. In this scanning electron micrograph, each diamond-shaped structure is the branched end of a group of four setae clustered together in a tetrad. (E) Toe peeling (digital hyperextension, DH) during detachment. Scale bars, 50 μm (D), 5 μm (A), 1 μm (B).

of the seta, causing fracture of the spatula–substrate bonds (Autumn et al., 2000) and returning the seta to the unloaded default state (Autumn and Hansen, 2006).

Macroscale peeling of toes

Macroscale detachment of adhesive pads occurs by digital hyperextension (DH; Fig. 1E) in both geckos (Autumn and Peattie, 2002; Russell, 1975; Russell, 2002) and frogs (Hanna and Barnes, 1991). The peeling motion of DH may reduce the force needed to overcome adhesion (Gay, 2002). This is well supported in frogs (Hanna and Barnes, 1991), where the mechanism of adhesion is primarily capillary force, and the pads are isotropic in function. Removal of adhesive tapes is done most easily by peeling since only a small region of interface must be separated at any given time. Prevention of peeling is important in the design of engineered adhesive joints, since flexibility in one or both contact surfaces will cause stress concentrations and result in crack propagation through the interface (Gay, 2002; Pocius, 2002).

Peeling model predictions

Models of peeling tape generally treat the adhesive surface as a continuum (Kendall, 1975). The force during peeling of a flexible strip of tape is given by:

$$F = bdE\left(\cos\alpha - 1 + \sqrt{\cos^2\alpha - 2\cos\alpha + 1 + 2R/dE}\right), \quad (1)$$

where b is the width of the strip, d is the thickness of the strip, E is material stiffness, R is the adhesion energy, and α is the peel angle. Consider a weight suspended from a strip of tape attached to a surface of angle α over vertical. Solving for α in Eqn 1, the angle (α^*) at the onset of peeling is

$$\alpha^* = \cos^{-1}\left(1 - \frac{bR}{F} + \frac{F}{2bdE}\right). \quad (2)$$

The peeling model predicts that greater weight will initiate peeling at shallower angles. Including the elastic stretch term,

maximum peeling force, which occurs at low angles, is limited by:

$$F_{\max} = \sqrt{2Rb^2dE}\,, \tag{3}$$

showing that stiffer materials, given the same adhesion energy, will peel at higher loads.

Peeling mechanics can apply – at least in theory – to fibrillar gecko-like materials (Hui et al., 2004). However, in real geckos where attachment is *via* a series of scansors bearing anisotropic setae, the validity of conventional (Kendall, 1975) peeling mechanics is less clear. Geckos hold their toes in a hyperextended position when not climbing – possibly protecting the scansors from abrasion (Russell, 1975), suggesting that DH could have functions other than reduction of detachment force *via* peeling mechanics. Indeed, it has been suggested that spatulae could detach more or less simultaneously (Gay, 2002), due to their mechanical independence. We tested the hypothesis of gecko pad detachment *via* peeling mechanics experimentally by measuring detachment angles of isolated setal arrays and live gecko toes, and evaluated the predictions of contact mechanical models of peeling using a computer simulation.

Materials and methods

Live geckos

Tokay geckos (*Gekko gecko* L.) are capable of supporting many times their body weight by a single toe. We discovered that the normally aggressive and temperamental tokays became docile when attached by a single toe to a glass surface. Using a goniometer stage (Newport, Irvine, CA, USA), we slowly ($<1^\circ\ s^{-1}$) increased the angle of a glass microscope slide to create an overhanging surface. We define the critical angle of detachment, α^*, as the angle over vertical at which detachment occurs. Using high speed video recording (500 frames s^{-1}) of the toe and goniometer, we measured α^* with a precision of $\pm1^\circ$ in 10 adult individuals (body mass=39.5±11.0 g, mean ± s.d.) attached by a single toe of the fore and hind limbs (Fig. 2). We attached cloth backpacks weighing 20, 50, 75 and 100 g to add weight to the animals. A thin strip of adhesive bandage tape (3M) acted as a muzzle to prevent bites. The muzzle left the nostrils unobstructed. A soft pad of bubble wrap cushioned falls. Animals were suspended a distance of approx. 10 cm above the pad, and in nearly all trials we caught the animal by hand prior to contact with the pad.

Isolated setal arrays

Specimen preparation

Tokay gecko (*Gekko gecko*) setal arrays were peeled from seven live adult animals as described previously (Hansen and Autumn, 2005). Test specimens were created by mounting the setal arrays to scanning electron microscope (SEM) stubs (product number 16261, Ted Pella, Redding, CA, USA) with cyanoacrylate adhesive (Loctite 410; Henkel Loctite Corp., Rocky Hill, CT, USA).

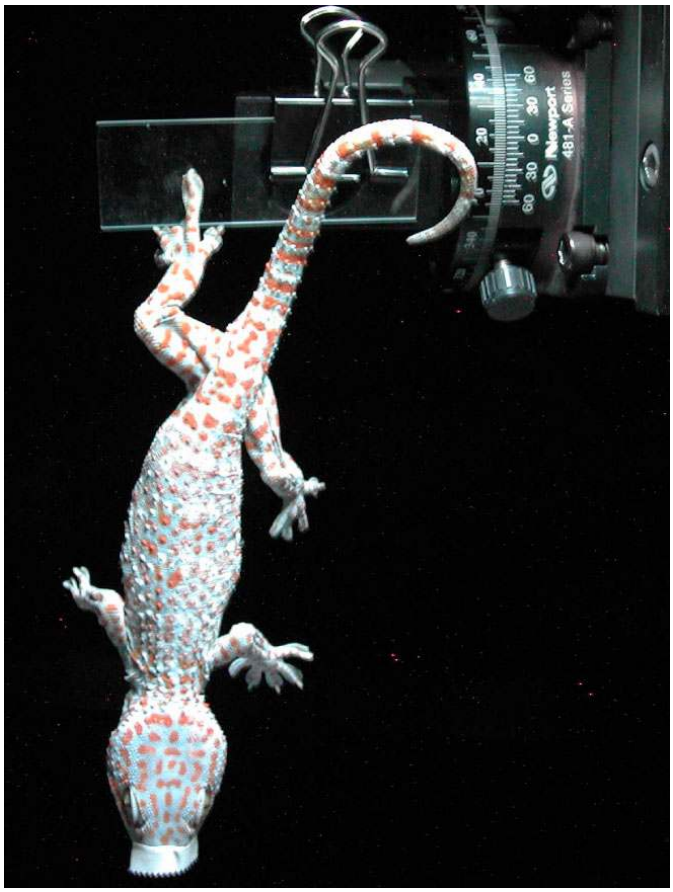

Fig. 2. Apparatus used to measure the angle (α^*) at which gecko toes detach from a glass surface. We discovered that the normally aggressive and temperamental tokays (*Gekko gecko*) became docile when attached by a single toe to a glass surface. A soft pad of bubble wrap cushioned falls. Animals were suspended a distance of approx. 10 cm above the pad, and in nearly all trials we caught the animal by hand prior to contact with the pad. A thin strip of adhesive bandage tape acted as a muzzle to prevent bites.

Mechanical testing apparatus

Setal array specimens were mounted on scanning electron microscope (SEM) stubs and evaluated with a custom two-axis mechanical tester. The specimen chuck was attached to a Kistler 9328A three-axis force sensor (Kistler, Winterthur, Switzerland) that was moved in the *z* (up-and-down) and *y* (left-and-right) axes with Newport 460P stages (Newport) driven by closed loop brushless DC servomotors (Newport 850G-HS actuator in the *y* axis and a Newport 850G actuator in the *z* axis). The stage and force sensor assembly were vertically mounted to a steel block above a 3 m × 0.9 m Newport RP Reliance breadboard table. A Newport ESP 300 servocontroller drove the actuators. Force measurements were collected through an AD Instruments Maclab/4e data acquisition unit (ADInstruments, Milford, MA, USA). The stage controller and force acquisition were interfaced with a Powerbook G3 (Apple Computer, Cupertino, CA, USA) for automated control of array experiments. Test substrates were held in place by toggle strap

clamps with spring plungers that bolted to the Newport breadboard table. Array test specimens were mounted in the mechanical tester chuck so that their natural path of drag was in alignment with the *y* axis. The array alignment was carried out with the help of a mirror.

The test substrate for the experiments was a glass microscope slide washed with de-ionized water and dried with Kimwipes (Kimberly-Clark, Neenah, WI, USA) before each test sequence. We used two types of experiments. (1) Testing setal arrays along the natural path of drag ('along setal curvature') assesses their adhesion and friction in the typical orientation geckos use them to climb (Autumn et al., 2000). (2) Pressing the setal arrays against the natural path of drag ('against setal curvature') tests them opposite to the usual direction for climbing, in which they do not adhere (Autumn et al., 2000). Tests were conducted with a crosshead speed of 50 μm s^{-1} in both the *z* axis and the *y* axis for all experiments, yielding frequencies of approx. 1 Hz.

Isolated setae

We used data of detachment angle α* as a function of adhesive force ($F_{\perp}$) collected in a previous study (Autumn et al., 2000), where pull-off force and shaft angle of isolated tokay setae were measured using optical deflection of a 4.7 mm long, 25 μm diameter aluminum bonding wire (American Fine Wire Corp., Selma, AL, USA). A flattened 50 μm×100 μm region was present at the wire tip. The seta was first preloaded perpendicular to the surface with a force of 1.6±0.25 μN (mean ± s.d.).

Statistics

We used SigmaPlot 9/SigmaStat 3.1 (Systat Software, Point Richmond, CA, USA) for all statistical analyses other than ANCOVA, for which we used StatView 5 (SAS Institute, Cary, NC, USA). We used Mathematica 5.1 (Wolfram Research, Inc., Champaign, IL, USA) for data filtering and reduction. Values are means ± s.e.m. unless otherwise stated.

Results

Critical angle of detachment in the toes of live geckos

Geckos attached to a glass slide by a single toe detached at an average angle (α*) of 25.5±0.2° (*N*=181). Median α* was 26.0°. The effect of mass on α* was not significant (ANCOVA, *F*=1.42; d.f.=1,177; $P \gg 0.05$), nor was the effect of the backpack (*F*=0.24; d.f.=1,177; *P*>0.05). The mean ratio between adhesion and friction was tan(25.5°)=0.477. The low variability in α* resulted in a highly linear relationship between adhesion and friction (shear force). The resolved adhesion and friction forces are $F_{\perp}=m\boldsymbol{g}\sin\alpha^*$ and $F_{\parallel}=m\boldsymbol{g}\cos\alpha^*$, respectively, where *m* is the total mass (body mass plus added mass of backpack), ***g*** is gravitational acceleration, and α* is the detachment angle. The linear regression of adhesive force on friction force was $F_{\perp}=-0.430F_{\parallel}+0.022$ (R^2=0.93), in N.

Friction and adhesion of isolated setal arrays

When dragged against their natural path (against curvature) setal arrays remained compressed and did not adhere (Fig. 3A). Average friction, $F_{\parallel}$, was 7.5±0.0004 mN (*N*=12), for an average normal (compressive) force, $F_{\perp}$ of 25.0±0.2 mN, yielding a friction coefficient, μ, of 0.31±0.02. When dragged along their natural path (with curvature) setal arrays compressed initially and then adhered, resulting in tensile normal forces (Fig. 3B). Average $F_{\parallel}$ in arrays dragged with curvature was 74.6±9.0 mN (*N*=25). Average adhesive force, $F_{\perp}$, was 34.8±4.6 mN. Adhesive force was a linear function of shear force: $F_{\perp}=-0.487F_{\parallel}+0.002$ (R^2=0.89), in N. The angle of the resultant force vector is $\alpha^*=\tan^{-1}(F_{\perp}/F_{\parallel})$. Using values of α* calculated from $F_{\perp}$ and $F_{\parallel}$ for each trial, average α* was 24.6±0.9°.

Critical angle of detachment in isolated setae

We used data collected earlier (Autumn et al., 2000) for the detachment angle (α*) of single setae. Average α* was 30.0° (s.e.m.=0.27°, *N*=60) and median was 30.1°. The mean ratio between adhesion and friction, the tangent of mean α*, in isolated setae is tan(30.0°)=0.577. The linear regression of adhesive force on friction force was $F_{\perp}=-0.597\ F_{\parallel}-1.20\times10^{-7}$ (R^2=0.98), in N.

Comparison of critical angle of detachment among seta, array and toe

α* values for single setae (Autumn et al., 2000) did not differ significantly from a normal distribution (Kolmogorov–Smirnov test of normality, D_{K-S}=0.066; *P*>0.2). α* values differed significantly from a normal distribution for arrays (D_{K-S}=0.216; *P*=0.004) and toes (D_{K-S}=0.135; *P*<0.001). For this reason we do not report parametric ANOVA statistics, but instead used a Kruskal–Wallis one-way analysis of variance of ranks. Note that the parametric ANOVA yielded similar results with respect to significance of differences in α* among seta, array, and toe levels. Values of α* differed significantly among seta, array and toe levels (Kruskal–Wallis, *H*=90.133; d.f.=2; *P*<0.001). Array and toe values of α* were not significantly different from each other (Dunn's pairwise contrasts, Δ_{rank}=4.475; *Q*=0.273; *P*>0.05), and were significantly lower than α* in setae (Δ_{rank}>103; *Q*>5.6; *P*<0.05).

Discussion

Friction

Gecko setae are a non-lubricated adhesive system based on van der Waals forces (Autumn et al., 2002), which suggests that their friction may be similar to that of typical dry solids. In the classical understanding of friction (Bhushan, 2002; Bowden and Tabor, 2001) of dry solids moving over one another, microscopic interference, welding and/or other bonding phenomena lead to the well known frictional relationship $F_{\parallel}=\mu F_{\perp}$, where μ is the coefficient of friction and $F_{\perp}$ is the normal force. When dragged across glass against their natural curvature, isolated arrays of gecko setae exhibit a

typical coefficient of friction of 0.31±0.02 (Fig. 3A,C), consistent with prior results (Autumn et al., 2006b).

Frictional adhesion

When dragged along their natural curvature, isolated setal arrays of geckos exhibit a very different tribological response than that predicted by previous friction/adhesion models or the Kendall tape peeling model (Eqn 1). As an array of setae began to slide along the surface, adhesion developed and persisted (Fig. 3B,D). Surprisingly, the ratio of shear force to adhesive force was approx. 2:1, irrespective of force magnitude (Fig. 4A). To test the generality of this effect, we measured the angle at detachment (α*) in live geckos hanging by a single toe. The angle at which toes detach was 25.5±0.2° (*N*=181), similar to α*=24.6±0.9° for isolated arrays. The peeling model predicts that larger forces cause lower values of α* (see Eqn. 2). Instead, gecko toes detached at a constant angle regardless of applied force. These results are consistent with the function of single isolated setae (Autumn et al., 2000), which detach at an angle of 30.0±0.27° (Fig. 4B). Indeed, it is likely that the value of α*=30° in single setae sets the upper limit for α* at the array and toe levels.

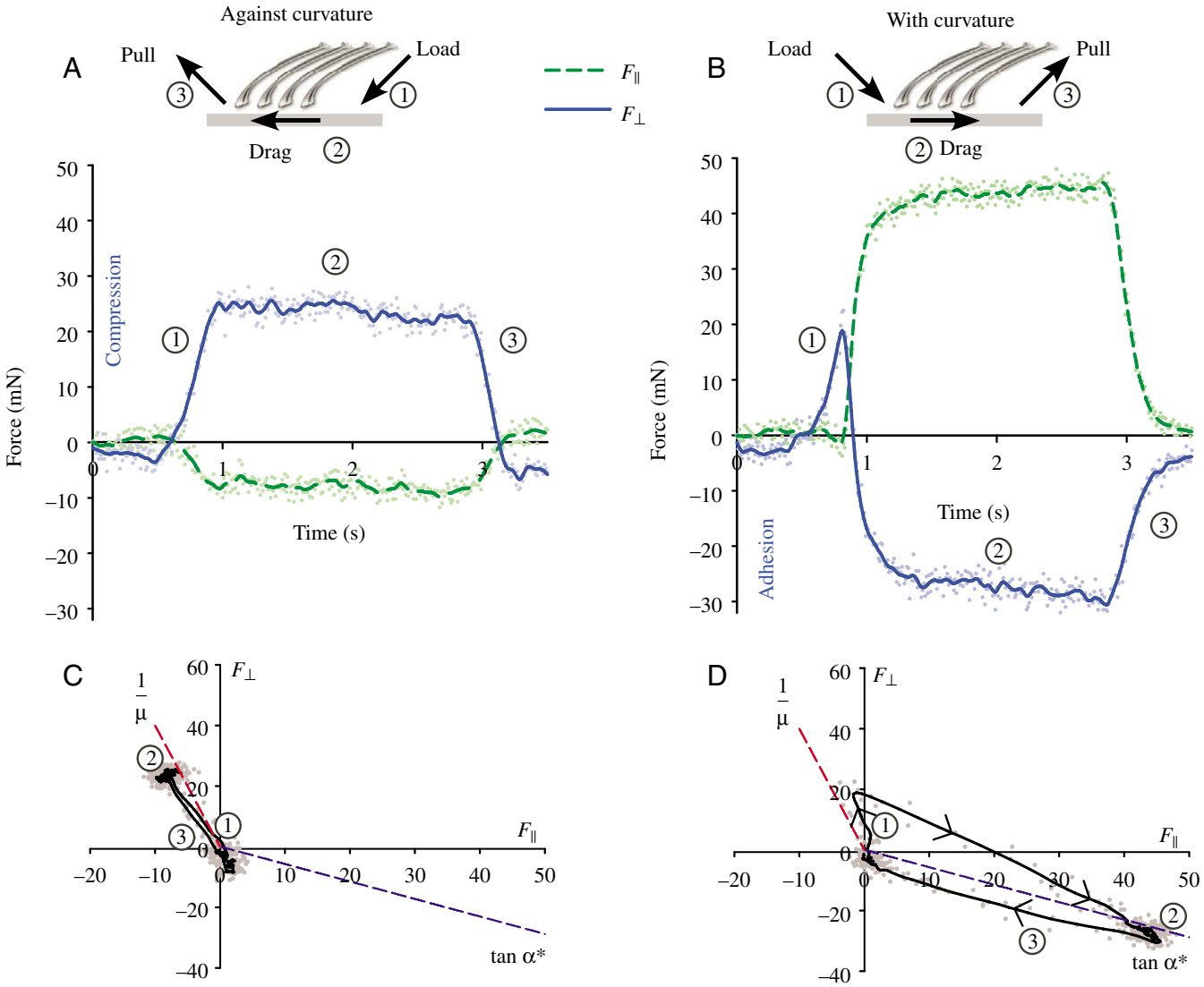

Fig. 3. Shear and normal forces in isolated gecko setal arrays on a glass surface. Motion in normal and shear axes was controlled at 50 μm s^{-1}. (A) Setal array during load (1), drag (2) and pull (3) (LDP) against the curvature of the setal shafts exhibits Coulomb friction. Negative $F_{\parallel}$ represents the reaction forces during a drag to the left. However, no difference between static and kinetic friction was evident. Compression force $F_{\perp}$ was approx. 3.2 times shear force $F_{\parallel}$. (B) Setal array during LDP with the curvature of the setal shafts compressed initially, and then was pulled into tension as the setal tips adhered. Positive $F_{\parallel}$ represents the reaction forces during a drag to the right. Adhesion was sustained during the 100 μm drag step (2). (C) Normal *vs* shear force during LDP against curvature of the setal shafts. $F_{\perp}$ and $F_{\parallel}$ followed a path along the Coulomb friction cone (red broken line of slope 1/μ). (D) Normal *vs* shear force during LDP with curvature of the setal shafts. $F_{\perp}$ and $F_{\parallel}$ followed a path that began initially along the Coulomb friction cone (red broken line of slope 1/μ). As adhesion developed, the forces converged on $F_{\perp}=-F_{\parallel}\tan\alpha^*$, where $\alpha^*\approx30°$ (blue broken line).

We now propose a simple model for the contact of a gecko foot describing the relationship between adhesive and shear forces, as shown by the results of this study. In the non-adhesive direction (against setal curvature; Fig. 3C), the Coulomb law governs friction:

$$F_{\perp} \geqslant -\frac{1}{\mu} F_{\parallel}\,, \tag{4}$$

which defines the minimum compressive load to withstand a given shear load. In the adhesive direction (with setal curvature; Fig. 3D), the adhesive force is limited by the shear force and the critical angle of detachment, α*. We term this new model 'frictional adhesion',

$$F_{\parallel} \geqslant -\frac{F_{\perp}}{\tan\alpha^*}\,, \tag{5}$$

which defines the minimum shear load to withstand a given adhesive load. Finally, we set an upper limit on the maximum shear force:

$$F_{\parallel} \leqslant F_{\parallel \mathrm{Max}}\,, \tag{6}$$

which will, in general, be a function of material strength, shear strength of the contact interface, and the maximum force that a limb can apply to the contact.

A test of the frictional adhesion model for gecko pads would be to measure the ratio of $F_{\parallel}$ to $F_{\perp}$ during actual climbing. Using values for α* of 25 to 30°, we predict a shear force greater than 1.7–2.1 times the adhesive force. A shear force of less than 1.7 times the adhesive force would fail to support the frictional adhesion model. While there are no force data for climbing tokay geckos, data do exist for climbing house geckos (*Hemidactylus garnotii*) (Autumn et al., 2006a). We reanalyzed the wall-reaction force data for the front legs of climbing house geckos from Autumn et al. (Autumn et al., 2006a) and found that average $F_{\parallel}$=0.030±0.004 N (*N*=13) and average $F_{\perp}$=0.006±0.002 N (*N*=12). Thus, shear force was 5 times adhesive force, suggesting that climbing geckos generated much greater shear forces than were required to maintain adhesion. The angle of the average resultant force vector during real climbing was $\tan^{-1}(F_{\perp}/F_{\parallel})$=11.3°, well below the 25 to 30° value of α* in toes, arrays and single setae in tokay geckos (*Gekko gecko*), consistent with the frictional adhesion model.

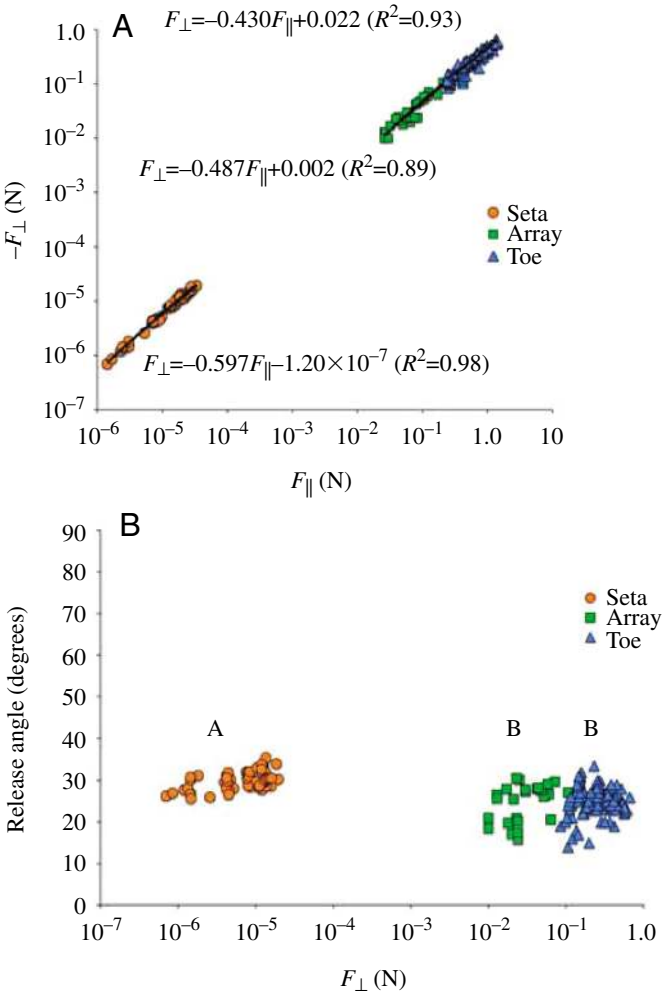

Fig. 4. (A) Adhesion ($-F_{\perp}$) *vs* shear force ($F_{\parallel}$) at three scales: isolated setae (circles), isolated setal arrays (squares) and live gecko toes (triangles). For all scales, $F_{\perp}=-F_{\parallel}\tan\alpha^*$, where $\alpha^*\approx30°$. (B) Release angle (α*) *vs* adhesion ($-F_{\perp}$) at three scales: isolated setae (circles), isolated setal arrays (squares) and live gecko toes (triangles). For all scales, α* was near 30°. Values of α* differed minimally but significantly among seta, array and toe levels (Kruskal–Wallis, *H*=90.133; d.f.=2; *P*<0.001). Letters A and B denote significant Dunn's pairwise contrasts. Array and toe values of α* were not significantly different from each other (Δ_{rank}=4.475; *Q*=0.273; *P*>0.05), and were significantly lower than α* in setae, suggesting that the value of α*=30° in single setae sets the upper limit for detachment angles at array and toe scales.

Table 1. *Contact model parameters for simulation of gecko attachment strategies*

Frictional adhesion	
Coefficient of friction, μ	0.25
Detachment angle, α*	25°
Positive shear limit, $F_{\parallel \mathrm{Max}}$	1.6 N
JKR	
Modulus of elasticity, *E*	2.5 MPa
Poisson ratio, υ	0.5
Adhesion energy, γ	58.5 mJ m^{-2}
Radius of curvature, *R*	5 mm
Number of contacts	215
Maximum shear stress, τ	21.7 kPa
Kendall peel	
Modulus of elasticity, *E*	2.5 MPa
Thickness, *d*	0.5 mm
Width, *b*	15 mm
Adhesion energy, *R*	5 J m^{-2}

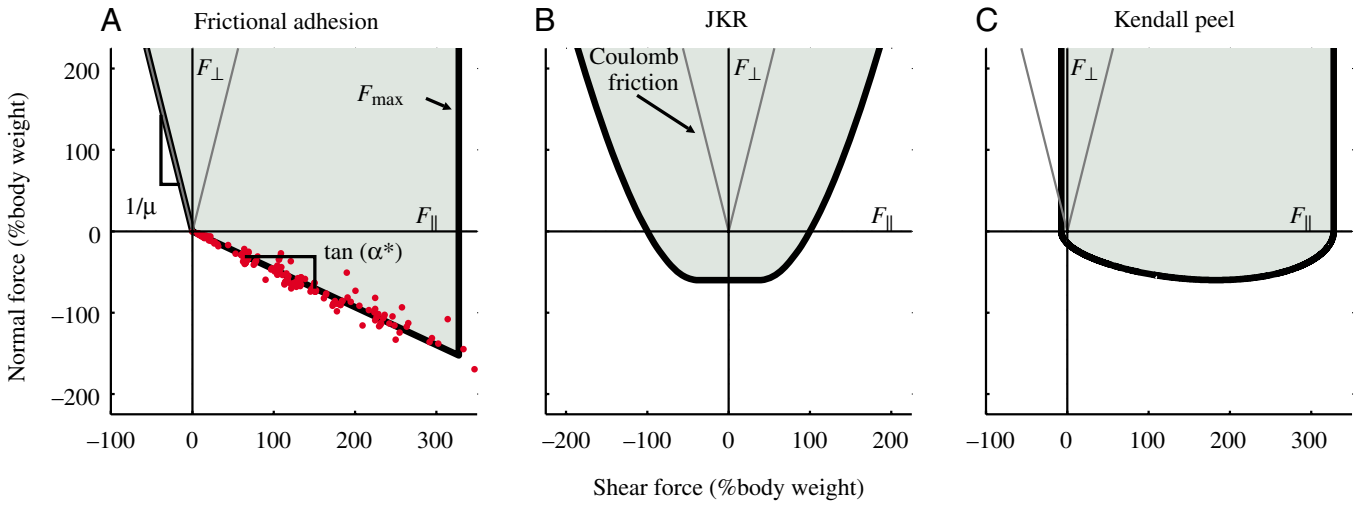

Fig. 5. Comparison of frictional adhesion, JKR and Kendall peel models. We chose parameters such that a 2-D model of a 50 g gecko could adhere to inclined planes from 0° to 180°. Stability regions (shaded) and limits (borders) of each model are plotted in force–space ($F_\parallel$, $F_\perp$) measured as a percentage of body weight. (A) Frictional adhesion given by Eqn 4, Eqn 5 and Eqn 6 along with current experimental results from setal arrays and toe detachment angles and previous results for single setae (Autumn et al., 2000). (B) JKR model for elastic spherical asperity in contact with flat substrate. Absolute values for adhesive and shear forces have been increased to comparable levels by assuming an array of contact asperities each contributing to overall adhesion and shear (Peressadko and Gorb, 2004). (C) Kendall peel model for thin adhesive films. Maximum force occurs at 0° (intersection with $+F_\parallel$-axis) and decreases as peel angle increases (measured below horizontal) towards 90° (intersection with $-F_\perp$-axis), eventually reaching a minimum finite value at 180°. Maximum shear for positive normal force is assumed to be independent of normal force and set at the Kendall peel model limits for 0° and 180°.

Comparison of JKR, Kendall peel and frictional adhesion models

In Fig. 5 we compare the frictional adhesion model (Fig. 5A) for the gecko pad and two commonly used adhesive models from the literature, the Johnson, Kendall, Roberts (JKR; Fig. 5B) model (Johnson et al., 1971) and the Kendall peel model (Fig. 5C) (Kendall, 1975). For each of these models we plotted a limit curve in force–space ($F_\parallel$, $F_\perp$). Combinations of normal and shear forces inside the shaded regions of Fig. 5 are safe; forces at the boundaries cause failure due to pull-off, sliding or peeling. We chose parameters for all three models to allow a 50 g model of a gecko to cling to an inclined plane at all angles between 0° (flat) and 180° (inverted). Table 1 contains a list of parameter values for the three contact models.

We used parameters for the Kendall peel model based on previous results for a micro-structured tape (Daltorio et al., 2005) and the original data (Kendall, 1975), using a constant adhesion energy. Adhesion energy is velocity-dependent in peeling tape (Crosby and Shull, 1999; Kendall, 1975); the adhesion energy used here corresponds to a near-zero peel velocity. At small peel angles, the maximum force is given by Eqn. 3. As peel angle increases to 90° (pulling away from the surface) and then to 180° (pulling back on itself) the peel force decreases. We consider onset of peeling as a failure of the contact. For positive normal forces, we assume the maximum shear force is independent of normal force and is given by the Kendall peel model limits at peel angles of 0° and 180°. A reasonable alternative would be to assume that the contact obeys the Coulomb friction limit (as shown in Fig. 5B) for positive normal forces.

The frictional adhesion (Fig. 5A) model parameters are derived from the results of this study. For purposes of comparison, we chose the shear force limit to coincide with that given by the peel model. However, as noted previously, a gecko is capable of supporting its entire weight by a single toe on a vertical surface (Autumn, 2006). Thus it is reasonable to expect that an entire gecko foot could support 3 or 4 times the gecko's weight, comparable to the limits on shear force in both the frictional adhesion and peel models used here.

We used the JKR model (Johnson et al., 1971) to calculate the adhesive and shear forces sustainable by a spherical elastic asperity in contact with a flat substrate. We chose parameters based on the results for an array of micro-structured posts (Peressadko and Gorb, 2004). To generate comparable amounts of adhesion to the previous models, we increased the number of posts in contact with the substrate and assumed the macroscopic behavior scales linearly. We calculated shear force using the contact area given by JKR, setting the maximum shear stress to 21 kPa, which is larger than values shown for rubber (Savkoor and Briggs, 1977), but reasonable for tacky materials. Johnson showed that shear loads below the slip limit (flat portion of the JKR curve in Fig. 5B) reduce the maximum pull-off force (Johnson, 1997). We neglected this effect because while it would round the flat portion of the JKR curve, there is no significant effect on the general characteristics of the model or our subsequent comparison and analysis.

In the tape peeling model (Fig. 5C), maximum pull-off force occurs when a positive shear force is also present; however, continued increase of shear force results in decreased pull-off

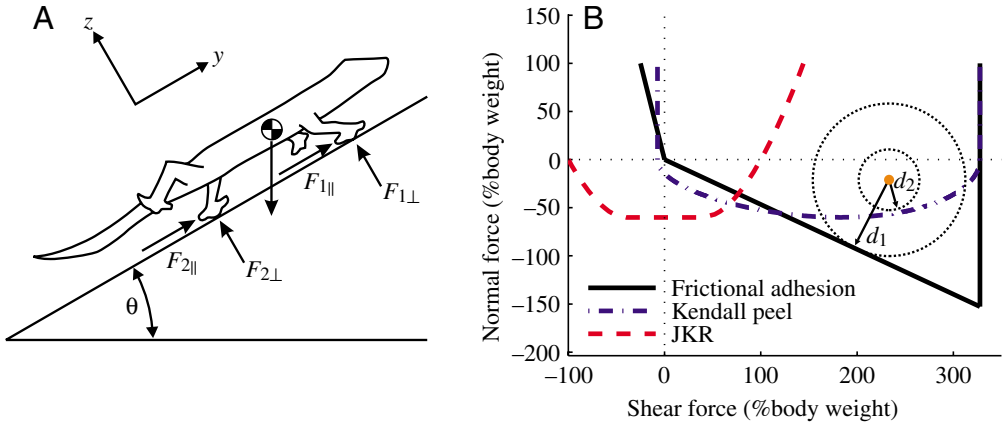

Fig. 6. (A) Planar model of a gecko on a flat inclined surface. θ is the angle of inclination and ranges from 0° (flat) to 180° (inverted). Center of mass was 2 cm above the surface and centered between the front and rear feet. A distance of 10 cm separated front and rear feet. For static equilibrium, forces in y and z and moment about x (not shown) must balance to zero. (B) Graphical description of stability margin. Given a particular point in force–space, the stability margin is shown using the frictional adhesion model (d_1) and the Kendall peel model (d_2). For the JKR model, the point shown would violate stability criteria and result in a negative stability margin. Stability margin is the minimum distance in *any* direction to avoid violating a constraint.

force due to stretching. The JKR model (Fig. 5B) has a maximum pull-off force when no shear force is present. In contrast, the frictional adhesion model (Fig. 5A) predicts that pull-off force increases linearly with shear load. Furthermore, frictional adhesion cannot sustain any pull-off force in the absence of shear whereas the peeling model shows a small pull-off force in the absence of shear. We argue that the requirement of shear force to maintain adhesion in the frictional adhesion model is an advantage for scansorial animals and robots – not a limitation – because it provides greater control over adhesive forces. Unlike the JKR and tape peeling models, the frictional adhesion limit curve intersects the origin. This allows a foot to separate from a surface with essentially zero contact forces at the actual instant of detachment, as reported in the experimental data (Autumn et al., 2006a). Non-zero forces at the instant before detachment cause force discontinuities when those forces drop rapidly to zero as detachment occurs. Force discontinuities cause disturbances of the center of mass and foot contact, potentially causing premature detachment or other undesirable behavior.

Model analysis

Each of the three contact models suggests a different strategy for the control of forces during climbing. Proper force-control strategies are important for the successful application of gecko-like adhesives to climbing robots (Autumn et al., 2005). A simplified planar model of a climbing gecko or robot, as shown in Fig. 6A, illustrates the implications of the different contact models. We adapted our analysis of the control of internal body forces (i.e. tension or compression forces between opposing feet, which do not affect the external force balance) from Kerr and Roth's work on dexterous manipulation (Kerr and Roth, 1986). The planar equations of static equilibrium require that forces in the y and z direction and moments about x axis sum to zero. However, the tangential and normal components of the contact forces at the front and rear foot represent four unknowns for the three equations of equilibrium, so one degree of freedom remains: the magnitude of the internal force between the front and rear foot: $F_{\mathrm{Int}}=F_{1\|}-F_{2\|}$. Positive values of F_{Int} indicate that the feet are pulling inward toward the center of mass.

For comparing the effects of contact model, we define a stability margin that represents the distance in force–space between a particular value of the contact forces, $\mathbf{F}_{\mathrm{i}}=(F_{\|},F_{\perp})$. at a particular foot and the nearest point, $f(x,y)$, on the corresponding limit curve for a contact model. The stability margin is then defined as

$$d_{\mathrm{i}} = \min \sqrt{(F_{\|}-x)^2 + (F_{\perp}-y)^2}\,, \qquad (7)$$

for all x and y on the limit curve. Fig. 6B shows a graphical representation of the stability margin for a particular point in force–space. It represents the largest magnitude perturbation force (measured as a percentage of body weight) that can be added, in any direction, to a foot without causing contact failure. In this analysis, we minimized the internal force while maintaining a minimum stability margin of 25% when possible.

When using an anisotropic model (Kendall peel model or frictional adhesion model), the foot orientation must be specified. For maximum stability the front foot is always oriented with the $+F_{\|}$ axis of the contact model aligned to the positive climbing direction, $+y$. For the rear foot, we tested both orientations ($+F_{\|}$ aligned with $+y$ or $-y$) for maximum stability. We performed our analysis numerically using Matlab 7 (The MathWorks, Inc., Natick, MA, USA). The center of mass was located 2 cm above the surface and centered between the front and rear feet. Front and rear feet were separated by 10 cm and the mass of the gecko was set at 50 g.

The results of the simulation (Fig. 7) predicted different strategies for distributing tangential loads depending on the

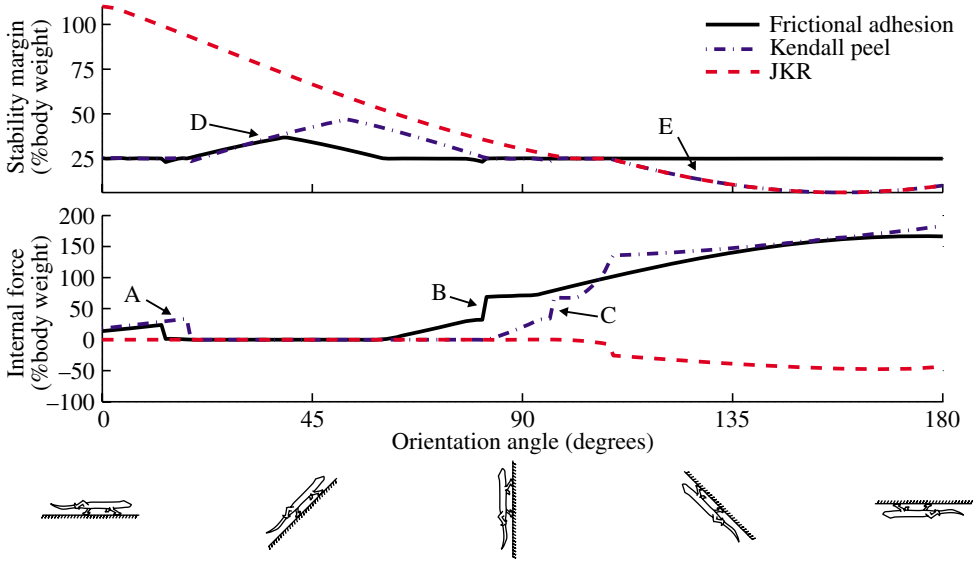

Fig. 7. The stability margin (top) and internal force (bottom) required for the gecko model to maintain a minimum stability margin of 25% body weight. Estimated force data from climbing house geckos, *Hemidactylus garnotii* (Autumn et al., 2006a), yielded a safety margin of approximately 36% body weight, assuming an α^* of 25°. Before point A, the frictional adhesion and Kendall peel models dictate the gecko orient its feet opposite of each other to maintain the specified stability margin. From point A to points B (frictional adhesion) and C (Kendall peel), the gecko model orients both feet with gravity since gravity naturally loads the contacts in their preferred adhesive direction and achieves greater than 25% stability margin (point D) without applying internal forces. As the surface becomes vertical and overhanging, the front foot must sustain more adhesion than the rear. In the JKR model, increasing adhesion is only possible by decreasing shear; thus, it is preferable for the rear foot to bear more shear load than the front. In the anisotropic models, the opposite is true. The front foot bears more shear load than the rear, because this tends to increase maximum adhesion. After points B and C, the respective anisotropic models only maintain the specified stability by reversing the rear foot and pulling inward with both feet. Point E indicates where both the peel and JKR models can no longer maintain the specified stability using any amount of internal force. This is in part due to the particular parameters chosen, but also due to the eventual decrease in adhesive forces when shear forces become too large.

contact model and inclination angle. For the isotropic JKR model, we found that the rear foot should always bear more of the shear load. Shear loads decreased adhesion in this model, so at inclines where the front foot requires more adhesion, the front foot was favored by assuming more tangential load on the rear foot. The frictional adhesion and tape peel models predicted the opposite strategy: the front foot should bear *more* shear load, thereby increasing its adhesion. The anisotropic models also resulted in different foot orientation preferences depending on surface inclination. Perhaps counterintuitively, on level surfaces the anisotropic models predicted that the feet should be opposed and pull inward for maximum stability. This makes the gecko resistant to perturbations that would tend to pluck it away from the surface as might occur if the gecko were attached to a moving horizontal surface such as a shaking leaf (Vinson and Vinson, 1969), or were seized by a predator (Hecht, 1952). The simulation predicted that when a gecko is inverted, the feet should be opposed and pull inward to remain adhered. Finally, although the frictional adhesion and peel models predicted similar trends, only the frictional adhesion model maintained the required stability margin over all inclines. While this result

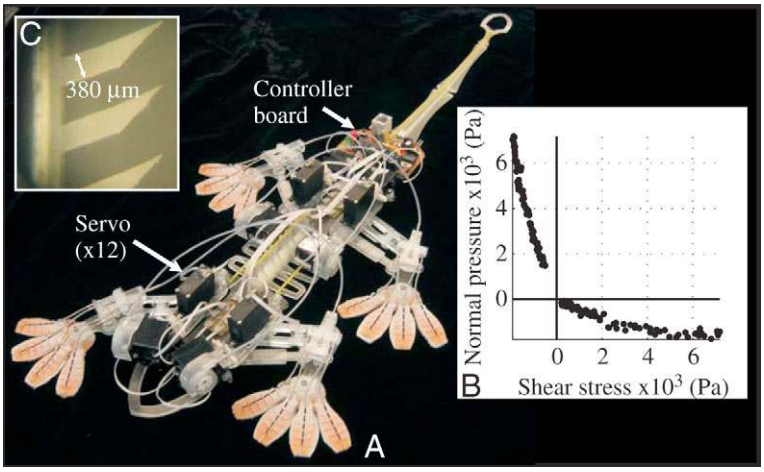

Fig. 8. Experimental climbing machine, 'Stickybot' (A), for testing anisotropic adhesive structures and force control strategies. Inset (B) shows experimental measurements of normal *vs* shear forces in an anisotropic frictional adhesive inspired by gecko setae. We used the same methods as for isolated gecko setal arrays. The urethane microarrays demonstrated a similar frictional adhesion response to that of gecko setae (Fig. 3D). Data were taken on a patch with an area of 35·mm^2. The area of each Stickybot toe is 431·mm^2 (C) Magnified view showing angled contact surface of frictional adhesive microarray.

is in part due to the material parameters chosen for the analysis (Table 1), it is also due to the details of the relationship between adhesive and shear forces at high tangential loads. This underscores the importance of the contact model and of properly controlling load distribution.

Conclusions

At the turn of the 20th century, Haase noted that attachment is load-dependent and only occurs in one direction: proximally along the axis of the toe (Haase, 1900). Hora observed that geckos generated adhesion only in combination with a shear force (Hora, 1923), leading him to conclude that geckos adhere by having a very large coefficient of friction. Subsequent workers (Autumn, 2006; Autumn et al., 2000; Dellit, 1934; Mahendra, 1941) dismissed Hora's hypothesis of adhesion-by-friction on the theoretical grounds that it could not explain how a gecko hangs on an inverted surface. With no load from gravity, friction should be absent, irrespective of the value of μ. However, our results and theory suggest that perhaps Hora was ahead of his time and that indeed geckos do adhere by using opposing feet to generate friction on inverted surfaces. In contrast to conventional friction (Eqn. 4), where the shear force is a function of the normal force, gecko setae represent a new phenomenon of 'frictional adhesion' where adhesion is a function of the shear force (Eqn. 5). This behavior is well-suited for climbing vertical surfaces since gravity naturally loads the contact in a way that generates adhesion. Frictional adhesion provides a means to control precisely the adhesion *via* the shear force, allowing attachment and detachment to occur with negligible forces (Autumn et al., 2006a).

It is unknown if the critical angle of detachment (α^*) is similar among species of gecko or precisely how morphological characteristics of the seta determine α^*. Further studies of setal structure and function will elucidate the mechanisms underlying frictional adhesion. Measuring kinematics and kinetics of geckos on vertical and inverted surfaces to yield foot orientation and internal forces will test the predictions of the frictional adhesion model and our simulation. Behavioral observations of geckos in nature will provide an important test of our stability predictions. For example, it is possible that when threatened by a predator (Hecht, 1952) geckos maximize adhesive stability by opposing the orientation of their feet and producing high internal shear forces. While setal structures in insects adhere with a liquid secretion, they may also be governed by a similar frictional adhesion relationship, as are gecko setae. Peak friction in whole insects on centrifuges is 5–11 times the peak adhesion (Gorb et al., 2002). A future study should explore the possibility that frictional adhesion occurs in insects and governs the control of leg forces in climbing insects (Niederegger and Gorb, 2003; Niederegger et al., 2002). Using the whole-insect friction:adhesion ratios of 5:11 (Gorb et al., 2001; Gorb et al., 2002) our model predicts critical angles of 11.3–5.2°, much lower than that of the gecko setae in our study. However, since multiple legs were in contact in these studies, one cannot resolve the angles of the adhesive patches at detachment.

The results of this study are being applied to the design of climbing robots. A newly developed climbing robot, Stickybot (Fig. 8A), uses gecko-inspired structures that, while crude in comparison to those of a gecko, exhibit similar anisotropic frictional adhesion (Fig. 8B). Compared to isotropic adhesive materials, we have observed smoother and faster climbing when utilizing the directional, microstructured, frictional adhesives (Fig. 8C) rather than flat adhesive pads, possibly due to lower attachment and detachment forces. Toe peeling in geckos [digital hyperextension, DH (Russell, 1975)] has also inspired the design of hyperextensible toes on robot feet. Before Stickybot employed frictional adhesive pads, force discontinuities during foot detachment often caused catastrophic failure – even with the use of hyperextensible peeling toes. Our results question the value of DH in detachment in gecko feet since frictional adhesion can in theory permit detachment of the toe pads with near-zero forces without peeling, simply by reducing the shear load. However, DH might be desirable for detachment on vertical and inverted surfaces where body weight loads toes in shear and causes frictional adhesion.

List of symbols

b	width
d	thickness
E	material stiffness
$\mathbf{F}$	contact force
$F_{\perp}$	normal force
$F_{\parallel}$	shear force, friction
F_{Int}	internal force
$\boldsymbol{g}$	gravitational acceleration
m	total mass
R	adhesion energy
α	angle
α^*	detachment angle
μ	coefficient of friction
θ	angle of inclination

We thank Bob Full, Nick Gravish, Jacob Israelachvili, Kevin Kendall, Sangbae Kim and Al Pocius for helpful discussions. Research was supported by DARPA N66001-03-C-8045, NSF-NIRT 0304730, DCI/NGIA HM1582-05-2022 grants, Emhart Corporation, and a gift from Johnson & Johnson Dupuy-Mitek Corp.

References

Autumn, K. (2006). Properties, principles, and parameters of the gecko adhesive system. In *Biological Adhesives* (ed. A. Smith and J. Callow), pp. 225-255. Berlin Heidelberg: Springer Verlag.

Autumn, K. and Hansen, W. (2006). Ultrahydrophobicity indicates a nonadhesive default state in gecko setae. *J. Comp. Physiol. A* doi:10.1007/s00359-006-0149-y.

Autumn, K. and Peattie, A. (2002). Mechanisms of adhesion in geckos. *Integr. Comp. Biol.* **42**, 1081-1090.

Autumn, K., Liang, Y. A., Hsieh, S. T., Zesch, W., Chan, W.-P., Kenny, W. T., Fearing, R. and Full, R. J. (2000). Adhesive force of a single gecko foot-hair. *Nature* **405**, 681-685.

Autumn, K., Sitti, M., Peattie, A., Hansen, W., Sponberg, S., Liang, Y. A., Kenny, T., Fearing, R., Israelachvili, J. and Full, R. J. (2002). Evidence for van der Waals adhesion in gecko setae. *Proc. Natl. Acad. Sci. USA* **99**, 12252-12256.

Autumn, K., Buehler, M., Cutkosky, M., Fearing, R., Full, R. J., Goldman, D., Groff, R., Provancher, W., Rizzi, A. A., Saranli, U. et al. (2005). Robotics in scansorial environments. *Proc. SPIE* **5804**, 291-302.

Autumn, K., Hsieh, S. T., Dudek, D. M., Chen, J., Chitaphan, C. and Full, R. J. (2006a). Dynamics of geckos running vertically. *J. Exp. Biol.* **209**, 260-272.

Autumn, K., Majidi, C., Groff, R., Dittmore, A. and Fearing, R. (2006b). Effective elastic modulus of isolated gecko setal arrays. *J. Exp. Biol.* **209**, 3558-3568.

Bhushan, B. (2002). *Introduction to Tribology*. New York: John Wiley.

Bowden, F. and Tabor, D. (2001). *The Friction and Lubrication of Solids. Oxford Classic Texts in the Physical Sciences*, Reprint edition. New York: Oxford University Press.

Crosby, A. J. and Shull, K. R. (1999). Adhesive failure analysis of pressure-sensitive adhesives. *J. Polym. Sci. B* **37**, 3455-3472.

Daltorio, K. A., Gorb, S., Peressadko, A., Horchler, A. D., Ritzmann, R. E. and Quinn, R. D. (2005). A robot that climbs walls using micro-structured polymer feet. In *Climbing and Walking Robots: Proceedings of the Eighth International Conference on Climbing and Walking Robots and the Support Technologies for Mobile Machines* (ed. M. O. Tokhi, G. S. Virk and M. A. Hossain), pp. 131-138. London: Springer.

Dellit, W.-D. (1934). Zur Anatomie und Physiologie der geckozehe. *Jena. Z. Naturw.* **68**, 613-656.

Gao, H. J., Wang, X., Yao, H. M., Gorb, S. and Arzt, E. (2005). Mechanics of hierarchical adhesion structures of geckos. *Mech. Mater.* **37**, 275-285.

Gay, C. (2002). Stickiness – some fundamentals of adhesion. *Integr. Comp. Biol.* **42**, 1123-1126.

Gorb, S., Gorb, E. and Kastner, V. (2001). Scale effects on the attachment pads and friction forces in syrphid flies (Diptera, Syrphidae). *J. Exp. Biol.* **204**, 1421-1431.

Gorb, S. N., Beutel, R. G., Gorb, E. V., Jiao, Y., Kastner, V., Niederegger, S., Popov, V. L., Scherge, M., Schwarz, U. and Vötsch, W. (2002). Structural design and biomechanics of friction-based releasable attachment devices in insects. *Int. Comp. Bio.* **42**, 1127-1139.

Haase, A. (1900). Untersuchungen über den bau und die entwicklung der haftlappen bei den geckotiden. *Arch. Naturgesch.* **66**, 321-345.

Hanna, G. and Barnes, W. J. P. (1991). Adhesion and detachment of the toe pads of tree frogs. *J. Exp. Biol.* **155**, 103-125.

Hansen, W. and Autumn, K. (2005). Evidence for self-cleaning in gecko setae. *Proc. Natl. Acad. Sci. USA* **102**, 385-389.

Hecht, M. K. (1952). Natural selection in the lizard genus Aristelliger. *Evolution* **6**, 112-124.

Hora, S. L. (1923). The adhesive apparatus on the toes of certain geckos and tree frogs. *J. Proc. Asiatic Soc. Bengal* **9**, 137-145.

Hui, C. Y., Glassmaker, N. J., Tang, T. and Jagota, A. (2004). Design of biomimetic fibrillar interfaces: 2. Mechanics of enhanced adhesion. *J. R. Soc. Interface* **1**, 12-26.

Johnson, K. L. (1997). Adhesion and friction between a smooth elastic spherical asperity and a plane surface. *Proc. R. Soc. Lond. A Math. Phys. Eng. Sci.* **453**, 163-179.

Johnson, K. L., Kendall, K. and Roberts, A. D. (1971). Surface energy and the contact of elastic solids. *Proc. R. Soc. Lond. A Math. Phys. Eng. Sci.* **324**, 310-313.

Kendall, K. (1975). Thin-film peeling – the elastic term. *J. Phys. D Appl. Phys.* **8**, 1449-1452.

Kerr, J. and Roth, B. (1986). Analysis of multifingered hands. *Int. J. Robot. Res.* **4**, 3-17.

Mahendra, B. C. (1941). Contributions to the bionomics, anatomy, reproduction and development of the Indian house gecko *Hemidactylus flaviviridis* Ruppell. Part II. The problem of locomotion. *Proc. Indian Acad. Sci. B* **13**, 288-306.

Niederegger, S. and Gorb, S. (2003). Tarsal movements in flies during leg attachment and detachment on a smooth substrate. *J. Insect Physiol.* **49**, 611-620.

Niederegger, S., Gorb, S. and Jiao, Y. (2002). Contact behaviour of tenent setae in attachment pads of the blowfly *Calliphora vicina* (Diptera, Calliphoridae). *J. Comp. Physiol. A* **187**, 961-970.

Peressadko, A. and Gorb, S. N. (2004). When less is more: experimental evidence for tenacity enhancement by division of contact area. *J. Adhes.* **80**, 247-261.

Pocius, A. V. (2002). *Adhesion and Adhesives Technology: An Introduction* (2nd edn). Munich: Hanser Verlag.

Russell, A. P. (1975). A contribution to the functional morphology of the foot of the tokay, *Gekko gecko* (Reptilia, Gekkonidae). *J. Zool. Lond.* **176**, 437-476.

Russell, A. P. (2002). Integrative functional morphology of the gekkotan adhesive system (Reptilia: Gekkota). *Integr. Comp. Biol.* **42**, 1154-1163.

Savkoor, A. R. and Briggs, G. A. D. (1977). The effect of tangential force on the contact of elastic solids in adhesion. *Proc. R. Soc. Lond. A* **356**, 103-114.

Sitti, M. and Fearing, R. S. (2003). Synthetic gecko foot-hair micro/nano structures as dry adhesives. *J. Adhes. Sci. Tech.* **17**, 1055-1073.

Spolenak, R., Gorb, S. and Arzt, E. (2005). Adhesion design maps for bio-inspired attachment systems. *Acta Biomater.* **1**, 5-13.

Vinson, J. and Vinson, J.-M. (1969). The saurian fauna of the Mascarene islands. *Bull. Maurit. Inst.* **6**, 203-320.